Article

Transition-State Analysis of the DNA Repair Enzyme MutY

Joe A. B. McCann, and Paul J. Berti

Crystal structure   Oxacarbenium ion intermediate   **Experimental transition state**

More About This Article

Additional resources and features associated with this article are available within the HTML version:

- Supporting Information
- Access to high resolution figures
- Links to articles and content related to this article
- Copyright permission to reproduce figures and/or text from this article

View the Full Text HTML

ACS Publications
High quality. High impact.

Transition-State Analysis of the DNA Repair Enzyme MutY

Joe A. B. McCann[§] and Paul J. Berti*[‡][§]

Department of Chemistry and Department of Biochemistry and Biomedical Sciences, McMaster University, 1280 Main Street West, Hamilton, ON, L8S 4M1, Canada

Received December 22, 2007; E-mail: berti@mcmaster.ca

Ⓦ **This paper contains enhanced objects available on the Internet at http://pubs.acs.org/jacs.**

Abstract: The transition state (TS) structure of MutY-catalyzed DNA hydrolysis was solved using multiple kinetic isotope effect (KIE) measurements. MutY is a base excision repair enzyme which cleaves adenine from 8-oxo-G:A mismatches in vivo, and also from G:A mismatches in vitro. TS analysis of G:A-DNA hydrolysis revealed a stepwise S_N1 ($D_N{}^*A_N{}^‡$) mechanism proceeding through a highly reactive oxacarbenium ion intermediate which would have a lifetime in solution of $<10^{-10}$ s. C−N bond cleavage is reversible; the *N*-glycoside bond breaks and reforms repeatedly before irreversible water attack on the oxacarbenium ion. KIEs demonstrated that MutY uses general acid catalysis by protonating N7. It enforces a 3′-*exo* sugar ring conformation and other sugar ring distortions to stabilize the oxacarbenium ion. Combining the experimental TS structure with the previously reported crystal structure of an abortive Michaelis complex elucidates the step-by-step catalytic sequence.

Introduction

Cells use base excision repair to maintain the integrity of their DNA in the face of constant chemical insults from the environment. MutY is a base excision repair enzyme, the last line of defense in the GO system which protects against 8-oxo-G (OG)[1] lesions, one of the most common forms of DNA damage.[2] OG codes like a T residue in DNA replication, preferentially base-pairing with A rather than the normal base, C. If the cell divides again, A pairs with T in the second round of DNA replication, resulting in an overall G → T mutation. MutY hydrolyzes adenine from OG:A mismatches (Scheme 1),[3] initiating a repair pathway that ultimately restores the original G:C base pair.[2,4] In humans, somatic G → T mutations in the adenomatous polyposis coli gene, characteristic of colorectal adenomas and cancer, have been linked to mutations in human MutY, hMYH.[5]

Under single turnover conditions, adenine is excised from OG:A mismatches with a rate constant of 16 min^{-1},[6] which

corresponds to 12 kcal/mol of transition state (TS) stabilization energy.[7] G:A mismatches are also substrates, with an excision rate constant of 1.6 min^{-1}. Steady-state rates are much lower because product release is rate-limiting. The active sites of the crystal structures of *Escherichia coli* MutY (eMutY)[8] and *Bacillus stearothermophilus* MutY (bMutY)[9] are almost identical. On the basis of these structures, both concerted S_N2[8] and stepwise S_N1[9] mechanisms have been proposed. In both mechanisms, the adenine leaving group is proposed to be protonated by eMutY_Glu37/bMutY_Glu43 (E37/43). General acid catalysis is a common but not universal feature of enzymatic purine hydrolysis.[10] In the stepwise mechanism, E37/43 would then deprotonate and activate the water nucleophile. The bMutY_D144N•(OG:A)-DNA crystal structure provided a detailed view of enzyme•substrate contacts;[9] however, understanding how those contacts function in catalysis requires elucidating MutY's catalytic mechanism in detail.

Nonenzymatic *N*-glycoside hydrolyses have been characterized in detail in (deoxy-)nucleosides and in DNA.[11,12] The reactions are acid-catalyzed even at the highest pH values

---

§ Department of Biochemistry and Biomedical Sciences.

‡ Department of Chemistry.

(1) Abbreviations: AP, apurinic site; bMutY, *Bacillus stearothermophilus* MutY; eMutY, *Escherichia coli* MutY; KIE, kinetic isotope effect; OG, 8-oxo-G; PAGE, polyacrylamide gel electrophoresis; TS, transition state; UDG, uracil DNA glycosylase.

(2) Fowler, R. G.; White, S. J.; Koyama, C.; Moore, S. C.; Dunn, R. L.; Schaaper, R. M. *DNA Repair* **2003**, *2*, 159–173.

(3) Shibutani, S.; Takeshita, M.; Grollman, A. P. *Nature* **1991**, *349*, 431–434.

(4) David, S. S.; Williams, S. D. *Chem. Rev.* **1998**, *98*, 1221–1261.

(5) Al-Tassan, N.; Chmiel, N. H.; Maynard, J.; Fleming, N.; Livingston, A. L.; Williams, G. T.; Hodges, A. K.; Davies, D. R.; David, S. S.; Sampson, J. R.; Cheadle, J. P. *Nat. Genet.* **2002**, *30*, 227–232. Sampson, J. R.; Jones, S.; Dolwani, S.; Cheadle, J. P. *Biochem. Soc. Trans.* **2005**, *33*, 679–683. Kastrinos, F.; Syngal, S. *Semin. Oncol.* **2007**, *34*, 418–424. Olschwang, S.; Blanche, H.; De Moncuit, C.; Thomas, G. *Genet. Test.* **2007**, *11*, 315–320.

(6) Chmiel, N. H.; Livingston, A. L.; David, S. S. *J. Mol. Biol.* **2003**, *327*, 431–443.

(7) Berti, P. J.; McCann, J. A. B. *Chem. Rev.* **2006**, *106*, 506–555.

(8) Guan, Y.; Manuel, R. C.; Arvai, A. S.; Parikh, S. S.; Mol, C. D.; Miller, J. H.; Lloyd, S.; Tainer, J. A. *Nat. Struct. Biol.* **1998**, *5*, 1058–1064.

(9) Fromme, J. C.; Banerjee, A.; Huang, S. J.; Verdine, G. L. *Nature* **2004**, *427*, 652–656.

(10) Singh, V.; Schramm, V. L. *J. Am. Chem. Soc.* **2006**, *128*, 14691–14696.

(11) Shapiro, R.; Danzig, M. *Biochemistry* **1972**, *11*, 23–29. Shapiro, R.; Kang, S. *Biochemistry* **1969**, *8*, 1806–1810. Zoltewicz, J. A.; Clark, D. F.; Sharpless, T. W.; Grahe, G. *J. Am. Chem. Soc.* **1970**, *92*, 1741–1749. Parkin, D. W.; Leung, H. B.; Schramm, V. L. *J. Biol. Chem.* **1984**, *259*, 9411–9417. Barnes, J. A.; Williams, I. H. *Chem. Commun.* **1996**, 193–194. Mentch, F.; Parkin, D. W.; Schramm, V. L. *Biochemistry* **1987**, *26*, 921–930. Berti, P. J.; Schramm, V. L. *J. Am. Chem. Soc.* **1997**, *119*, 12069–12078. Schroeder, G. K.; Wolfenden, R. *Biochemistry* **2007**, *46*, 13638–13647.

(12) Parkin, D. W.; Schramm, V. L. *Biochemistry* **1987**, *26*, 913–920.

Scheme 1

(OG:A)-DNA → MutY / H₂O → AP-DNA + adenine
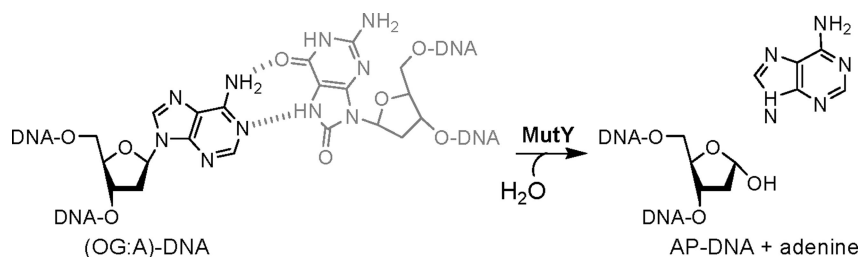
examined. The potential catalytic effect of protonating N7 of adenine has been estimated to be ~2 × 10⁵-fold, corresponding to a 7 kcal/mol decrease in activation energy.[7] Recent TS analysis of acid-catalyzed dAMP hydrolysis demonstrated N7 protonation and an S_N1 mechanism. It was predominantly a $D_N*A_N^{\ddagger}$ mechanism, with the *N*-glycoside bond breaking and reforming repeatedly, and with the first irreversible step being water attack on the oxacarbenium ion intermediate 80% of the time, or diffusional separation of adenine and the oxacarbenium ion 20% of the time.[13]

TS analysis involves measuring multiple kinetic isotope effects (KIEs) to determine the TS structure with sub-Ångstrom resolution.[7,14] KIEs report on changes in molecular structure between the reactant and the transition state. If a bond becomes weaker at the transition state, the light isotope will react faster, $^{\text{light}}k/^{\text{heavy}}k > 1.0$, giving a normal KIE. If the bond becomes stronger, the heavy isotope will react faster, $^{\text{light}}k/^{\text{heavy}}k < 1.0$, giving an inverse KIE. KIEs also reflect the reaction coordinate motion, and thus show which atoms are in motion at the transition state. KIEs are the most direct and detailed experimental approach to TS structure.

TS analyses of glycosylase reactions, most frequently with small molecule substrates,[15] have provided the detailed knowledge of enzymatic transition states that has made it possible to design dozens of pM to fM inhibitors,[16,17] including compounds that are in clinical trials for treatment of T-cell malignancies, transplant rejection, and autoimmune disease.[18] Most ribonucleoside reactions proceed through highly dissociative S_N2 mechanisms where leaving group departure is far advanced over nucleophile approach, resulting in the sugar ring having high

oxacarbenium ion (cationic) character at the transition state.[7] Recently, a few stepwise mechanisms with a discrete oxacarbenium ion intermediate have been observed.[10,19,20] TS analyses of two nucleic acid glycosylases have been reported: the uracil DNA glycosylase (UDG) reaction,[21] and ricin-catalyzed hydrolysis of adenine from RNA[22] and DNA.[23] These reactions proceeded through stepwise S_N1 mechanisms, while thymidine phosphorylase[24] proceeded through an almost synchronous S_N2 mechanism with essentially no cationic character at the transition state.

Using multiple KIEs, we show here that eMutY employs a stepwise S_N1 mechanism where the C−N bond repeatedly breaks and reforms before irreversible attack by the water nucleophile, a $D_N*A_N^{\ddagger}$ mechanism. TS analysis provides a powerful description of catalysis, particularly when combined with the bMutY_D144N•(OG:A) crystal structure.

Materials and Methods

Enzymes and Oligonucleotides. eMutY was produced as previously described.[25] Unlabeled oligonucleotides were purified by denaturing 30% PAGE with 7 M urea, 89 mM Tris, 89 mM boric acid, 2 mM EDTA.

Labeled GA25 Synthesis. The substrate GA25 was synthesized using 1150 U of murine leukemia virus reverse transcriptase (Invitrogen), 30 μM each of primer and template oligonucleotides, 26 μM of labeled dATPs[13] (1.4 × 10⁶ counts per minute (cpm) each of ¹⁴C and ³H) in 1000 μL of 50 mM Tris-HCl, pH 8.3, 75 mM KCl, 3 mM MgCl₂, and 10 mM dithiothreitol at 37 °C for 2 h (Figure 1). Unlabeled dATP, TTP, and dGTP (200 μM each) were added, and the reaction continued for 2 h. The volume was reduced 5-fold by lyophilization and DNA was precipitated with 3 volumes of ice cold absolute ethanol. The pellet was dissolved in 100 μL of water and desalted on a Microspin G-25 column (GE Healthcare). The strand was PAGE purified as above (Figure S3, S4). Overall radioactive yields were 20 to 60%.

Rate Assays. Hydrolysis of ³³P-labeled GA25 (³³GA25) was measured as described previously,[25] with 50 nM ³³GA25, 25 nM eMutY, and 9.3 nM hAPE1 (human apurinic/apyriminidic endonuclease 1, New England Biolabs) in buffer A: 20 mM potassium phosphate, pH 7.6, 30 mM KCl, 10 mM MgCl₂, 0.1 mg/mL bovine serum albumin. The solvent deuterium KIE was measured in the same way, but with 20 nM ³³GA25 and 40 nM eMutY in either H₂O or D₂O.

(13) McCann, J. A. B.; Berti, P. J. *J. Am. Chem. Soc.* **2007**, *129*, 7055–7064.

(14) Schramm, V. L. *Acc. Chem. Res.* **2003**, *36*, 588–596.

(15) Schramm, V. L. *Curr. Opin. Struct. Biol.* **2005**, *15*, 604–613.

(16) Ting, L. M.; Shi, W.; Lewandowicz, A.; Singh, V.; Mwakingwe, A.; Birck, M. R.; Ringia, E. A.; Bench, G.; Madrid, D. C.; Tyler, P. C.; Evans, G. B.; Furneaux, R. H.; Schramm, V. L.; Kim, K. *J. Biol. Chem.* **2005**, *280*, 9547–9554. Singh, V.; Evans, G. B.; Lenz, D. H.; Mason, J. M.; Clinch, K.; Mee, S.; Painter, G. F.; Tyler, P. C.; Furneaux, R. H.; Lee, J. E.; Howell, P. L.; Schramm, V. L. *J. Biol. Chem.* **2005**, *280*, 18265–18273. Lee, J. E.; Singh, V.; Evans, G. B.; Tyler, P. C.; Furneaux, R. H.; Cornell, K. A.; Riscoe, M. K.; Schramm, V. L.; Howell, P. L. *J. Biol. Chem.* **2005**, *280*, 18274–18282. Kicska, G. A.; Long, L.; Horig, H.; Fairchild, C.; Tyler, P. C.; Furneaux, R. H.; Schramm, V. L.; Kaufman, H. L. *Proc. Natl. Acad. Sci. U.S.A.* **2001**, *98*, 4593–4598. Miles, R. W.; Tyler, P. C.; Evans, G. B.; Furneaux, R. H.; Parkin, D. W.; Schramm, V. L. *Biochemistry* **1999**, *38*, 13147–13154.

(17) Lewandowicz, A.; Tyler, P. C.; Evans, G. B.; Furneaux, R. H.; Schramm, V. L. *J. Biol. Chem.* **2003**, *278*, 31465–31468.

(18) Balakrishnan, K.; Nimmanapalli, R.; Ravandi, F.; Keating, M. J.; Gandhi, V. *Blood* **2006**, *108*, 2392–2398. Ravandi, F.; Gandhi, V. *Expert Opin. Investig. Drugs* **2006**, *15*, 1601–1613. Gandhi, V.; Kilpatrick, J. M.; Plunkett, W.; Ayres, M.; Harman, L.; Du, M.; Bantia, S.; Davisson, J.; Wierda, W. G.; Faderl, S.; Kantarjian, H.; Thomas, D. *Blood* **2005**, *106*, 4253–4260. Gaweco, A. S.; Kilpatrick, M.; Bantia, S. *Transplantation* **2006**, *82*, 863–864.

(19) Lewandowicz, A.; Schramm, V. L. *Biochemistry* **2004**, *43*, 1458–1468.

(20) Singh, V.; Lee, J. E.; Nunez, S.; Howell, P. L.; Schramm, V. L. *Biochemistry* **2005**, *44*, 11647–11659.
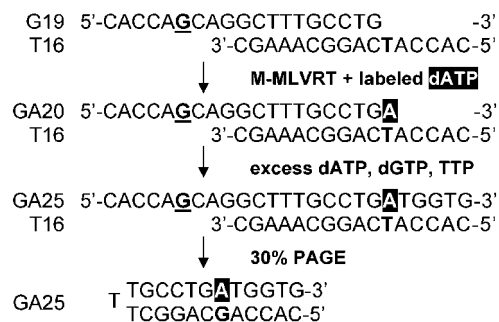
(21) Werner, R. M.; Stivers, J. T. *Biochemistry* **2000**, *39*, 14054–14064.

(22) Chen, X.-Y.; Berti, P. J.; Schramm, V. L. *J. Am. Chem. Soc.* **2000**, *122*, 1609–1617.

(23) Chen, X.-Y.; Berti, P. J.; Schramm, V. L. *J. Am. Chem. Soc.* **2000**, *122*, 6527–6534.

(24) Birck, M. R.; Schramm, V. L. *J. Am. Chem. Soc.* **2004**, *126*, 2447–2453.

(25) Porello, S. L.; Leyes, A. E.; David, S. S. *Biochemistry* **1998**, *37*, 14756–14764.

G19 5'-CACCA**G**CAGGCTTTGCCTG   -3'
T16   3'-CGAAACGGAC**T**ACCAC-5'

↓ **M-MLVRT + labeled dATP**

GA20 5'-CACCA**G**CAGGCTTTGCCTG**A**   -3'
T16   3'-CGAAACGGAC**T**ACCAC-5'

↓ **excess dATP, dGTP, TTP**

GA25 5'-CACCA**G**CAGGCTTTGCCTG**A**TGGTG-3'
T16   3'-CGAAACGGAC**T**ACCAC-5'

↓ **30% PAGE**

GA25 T TGCCTG**A**TGGTG-3'
       TCGGAC**G**ACCAC-5'

Figure 1. Synthesis of the GA25 stem-loop substrate. Labeled dATP and dAdo are in reverse type. The G of the G:A mismatch is underlined.
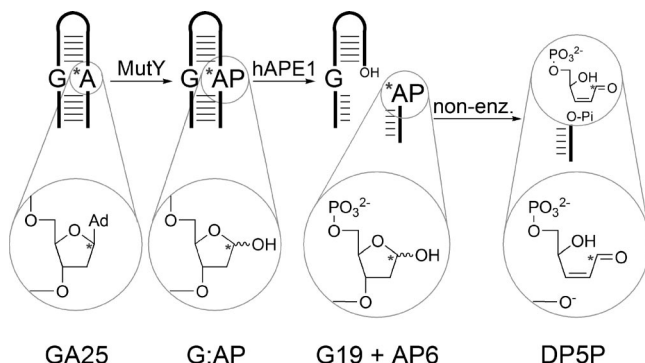
Figure 2. GA25 digestion during KIE measurements. Nonenzymatic elimination of DP5P largely occurs spontaneously during the MutY reaction, then is taken to completion with the NaOH quench. Ad = adenine, AP = apurinic site, DP5P = 4,5-dihydroxy-pent-2-enal 5-phosphate, * = radiolabeled position.

Commitment to Catalysis. Experimental KIEs reflect the first irreversible step of a reaction. It is therefore necessary to demonstrate that substrate binding is reversible before interpreting the KIEs in terms of the chemical steps. Commitment to catalysis, C_f, was determined by modifying Rose's isotope trapping method[26] for conditions where [enzyme] > [substrate] (see Supporting Information).

KIE Measurements. KIEs were measured using the competitive method[27] and the equation from ref 13 to calculate KIEs from isotope ratios. ^{3}H- and ^{14}C-labeled GA25's (4 μM, 2 × 10^5 cpm each of ^{3}H and ^{14}C), were combined in 900 μL of buffer A and divided into a partial reaction aliquot (600 μL) and a complete reaction aliquot (300 μL). eMutY was added (20 nM for partial reactions, 500 nM for complete), plus 9 nM hAPE1 (300 U/mL), and the reactions were incubated overnight at 37 °C. NaOH (130 mM) and 40 mM EDTA were added to quench the reaction and cleave any remaining G:apurinic (G:AP)-DNA product (Figure 2). The AP6 and DP5P products were purified in three equal portions by anion exchange chromatography (Mono-Q 5/5 HR column, GE Healthcare) (Figure S5). The products were eluted with 4.5 mL of 10 mM NaOH, 660 mM NaCl at 1.5 mL/min, and collected directly

(26) Rose, I. W. *Methods Enzymol.* **1980**, *64*, 47–59.
(27) Parkin, D. W. In *Enzyme mechanism from isotope effects*; Cook, P. F., Ed.; CRC Press Inc.: Boca Raton, 1991; p 269–290.
(28) Sponer, J.; Jurecka, P.; Hobza, P. *J. Am. Chem. Soc.* **2004**, *126*, 10142–10151. Kielkopf, C. L.; Ding, S.; Kuhn, P.; Rees, D. C. *J. Mol. Biol.* **2000**, *296*, 787–801. Soler-Lopez, M.; Malinina, L.; Liu, J.; Huynh-Dinh, T.; Subirana, J. A. *J. Biol. Chem.* **1999**, *274*, 23683–23686. Soler-Lopez, M.; Malinina, L.; Subirana, J. A. *J. Biol. Chem.* **2000**, *275*, 23034–23044. Sines, C. C.; McFail-Isom, L.; Howerton, S. B.; VanDerveer, D.; Williams, L. D. *J. Am. Chem. Soc.* **2000**, *122*, 11048–11056. Zhanpeisov, N. U.; Leszczynski, J. *J. Phys. Chem. A* **1998**, *102*, 6167–6172. Kumar, A.; Mishra, P. C.; Suhai, S. *J. Phys. Chem. A* **2005**, *109*, 3971–3979. Kabelac, M.; Zendlova, L.; Reha, D.; Hobza, P. *J. Phys. Chem. B* **2005**, *109*, 12206–12213.

Table 1. KIEs for eMutY-Catalyzed GA25 Hydrolysis

label of interest[a]	type of KIE	experimental KIE[b]	H+-catalyzed dAMP hydrolysis[d]
1'-^{14}C	primary ^{14}C	1.009 ± 0.003 (4)	1.004
9-^{15}N	primary ^{15}N	1.025 ± 0.001 (3)	1.022
7-^{15}N	secondary ^{15}N	0.992 ± 0.003 (4)	0.985
1'-^{3}H	α-secondary ^{3}H	1.150 ± 0.002 (2)[c]	1.253
2'S-^{2}H	β-secondary ^{2}H	1.091 ± 0.002 (4)	1.113
2'R-^{2}H	β-secondary ^{2}H	1.077 ± 0.001 (3)	1.091
6-^{15}N	secondary ^{15}N	1.011 ± 0.002 (3)	0.997
5',5'-^{3}H$_2$	α-secondary ^{3}H	0.968 ± 0.001 (3)	1.012

^{a} The 1'-^{3}H and 5',5'-^{3}H$_2$ KIE measurements used [5'-^{14}C]GA25 as the remote label, with the 5'-^{14}C KIE defined as unity. The ^{15}N and ^{2}H KIEs used 5'-^{14}C as a reporter radionuclide (e.g., [9-^{15}N,5'-^{14}C]GA25), and [5',5'-^{3}H$_2$]GA25 as the remote label. ^{15}N, ^{2}H, and the 1'-^{14}C KIEs were corrected using: KIE$_{corrected}$ = KIE$_{observed}$ × [5',5'-^{3}H$_2$]KIE. ^{b} Errors are the 95% confidence intervals. The number of independent KIE measurements is in parentheses. KIEs were corrected for incomplete labeling with stable isotopes.[13] ^{c} Average of two experiments. The difference between the two experiments is shown. ^{d} From reference 13; 95% confidence intervals are similar to the MutY-reaction.

into a plastic scintillation vial, then residual GA25 substrate was eluted with 4.5 mL of 10 mM NaOH, 1.1 M NaCl. Eluted fractions were neutralized with 0.25 mL of 1 M potassium phosphate, pH 6.0, and split into two vials. The liquid weights of the fractions were equalized using neutralized elution buffer, then 20 mL of scintillation fluid (Liquiscint, National Diagnostics) was added. Scintillation counting and measurement of the extent of reaction were as described previously.[13,27]

Computational Structures and Isotope Effects. Electronic structure optimizations, frequency, and KIE calculations were performed as described previously.[13] The G(*anti*):A(*anti*) reactant model, **2**, was based on previous computational models[28–30] and DNA hydration surveys.[29] The *anti:anti* conformation predominates in NMR and X-ray structures.[29–31] Intermediate and TS models (**4‡** to **9**) were based on the geometries of **3**, the flipped dAdo in the bMutY_D144N:(OG:A) structure.[9]

Results

KIE Measurement. KIEs were measured for eMutY-catalyzed hydrolysis of GA25, a G:A mismatch-containing substrate (Table 1). KIEs were measured by the competitive method,[27] that is, the heavy and light isotopes at the position of interest are present in the same reaction mixture and act as competitive substrates. Under these conditions, KIEs reflect the first irreversible step of the reaction, rather than the rate-limiting step.[7] hAPE1 was added to the reaction mixture to cleave the (G:AP)-DNA product on the 5' side of the AP site, releasing a radiolabeled 6 nt strand (AP6, Figure 2).[32] The radiolabeled β-elimination product, DP5P, and AP6 were purified from residual substrate by anion exchange chromatography, and the ^{3}H:^{14}C ratios were measured to yield the KIEs.

Commitment to Catalysis, C_f. The C_f was 0.028 ± 0.002 (see Supporting Information). This showed that catalysis was much

(29) Schneider, B.; Berman, H. M. *Biophys. J.* **1995**, *69*, 2661–2669.
(30) Schneider, B.; Cohen, D.; Berman, H. M. *Biopolymers* **1992**, *32*, 725–750. Schneider, B.; Cohen, D. M.; Schleifer, L.; Srinivasan, A. R.; Olson, W. K.; Berman, H. M. *Biophys. J.* **1993**, *65*, 2291–2303.
(31) Patel, D. J.; Kozlowski, S. A.; Ikuta, S.; Itakura, K. *Biochemistry* **1984**, *23*, 3207–3217. Li, Y.; Zon, G.; Wilson, W. D. *Biochemistry* **1991**, *30*, 7566–7572. Gao, X. L.; Patel, D. J. *J. Am. Chem. Soc.* **1988**, *110*, 5178–5182. Sanchez, A. M.; Volk, D. E.; Gorenstein, D. G.; Lloyd, R. S. *DNA Repair* **2003**, *2*, 863–878. Greene, K. L.; Jones, R. L.; Li, Y.; Robinson, H.; Wang, A. H. J.; Zon, G.; Wilson, W. D. *Biochemistry* **1994**, *33*, 1053–1062.
(32) Wilson, D. M.; Barsky, D. *Mutat. Res. DNA Repair* **2001**, *485*, 283–307.
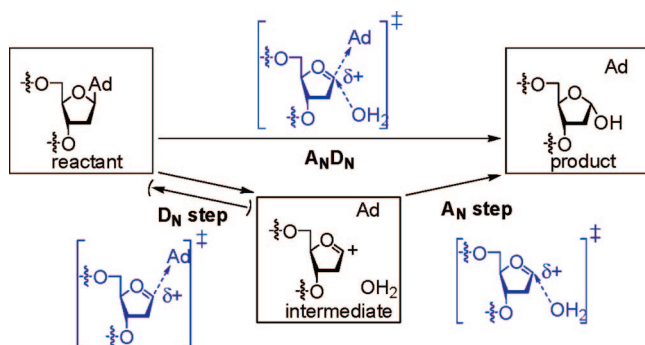
slower than substrate dissociation and therefore that the experimental KIEs reflected the chemical steps rather than substrate binding or other nonchemical steps. C_f values <0.05 are considered negligible.[22]

Description of Mechanisms. Because TS analysis can distinguish between three distinct S_N1 transition states, it is necessary to use IUPAC nomenclature.[33] *N*-glycoside hydrolysis can proceed through an S_N2 (or A_ND_N) transition state, with nucleophile approach (A_N) and leaving group departure (D_N) occurring in a single, concerted step (Scheme 2).[33] Alternatively, it can proceed through a stepwise S_N1 (or D_N*A_N) mechanism. The asterisk indicates an intermediate with a finite lifetime between leaving group departure (D_N) and nucleophile approach (A_N). $D_N^{\ddagger}*A_N$ is a reaction where leaving group departure is irreversible, while $D_N*A_N^{\ddagger}$ indicates that the C−N bond breaks and reforms repeatedly before final, irreversible nucleophile addition to complete the reaction. Reversible C−N bond breakage followed by an isotopically insensitive irreversible step is a "$D_N*?^{\ddagger}$" mechanism, as observed with ricin with an RNA substrate.[22] The unknown step could be, for example, a protein conformational change, dissociation of the leaving group from the active site, or water diffusion into position to attack the oxacarbenium ion.

KIE Calculation. KIEs are calculated from the vibrational frequencies of computational models.[34] It is not possible to derive a TS structure directly from the experimental KIEs; rather, KIEs are calculated for candidate TS structures and compared with the experimental KIEs.[7,34] As enzymes often stabilize different transition states from the corresponding nonenzymatic reaction, there is no guarantee that the computational transition states will match the real reaction. However, because vibrational frequencies from hybrid DFT calculations accurately reflect molecular structure, incorrect computational TS structures would have yielded computational KIEs that did not match the experimental values.[35] In that case, bond order vibrational analysis would have been needed to interpret the KIEs.[34] The match of calculated to experimental KIEs is good evidence that $8a^{\ddagger}/8b^{\ddagger}$ match the true transition state.

Computational TS structures were found for each potential mechanism (Figure 3), including: an A_ND_N transition state ($4^{\ddagger}$), a stepwise mechanism where C−N bond cleavage is irreversible, $D_N^{\ddagger}*A_N$ ($5^{\ddagger}$), or where water attack on the intermediate is the first irreversible step, $D_N*A_N^{\ddagger}$ ($8^{\ddagger} + 7$). Two similar transition states were found for the A_N step, $8a^{\ddagger}$ and $8b^{\ddagger}$, as observed

previously.[13] The observable KIEs for a "$D_N*?^{\ddagger}$" mechanism would equal the equilibrium IEs (EIEs) for forming intermediates **6** and **7**.[23]

The reactant model **2** was hydrogen bonded to guanine, with the conformation about the C4′−C5′ bond matching oligonucleotide crystal structures. Hydrogen bonding, hydration, and conformations all had observable effects on the calculated KIEs compared with simple dAdo as the reactant (**1**, Table S6). The conformations of **3**− **9** corresponded to the bMutY_D144N•(OG: A) crystal structure.[9]

Experimental Transition State. The best match of calculated to experimental KIEs was for a stepwise $D_N*A_N^{\ddagger}$ mechanism (Table 2). The calculated heavy atom KIEs for a $D_N*A_N^{\ddagger}$ mechanism, particularly $1'$-^{14}C, clearly matched the experimental values better than other mechanisms, and were all within 0.003 of the experimental values. In this mechanism the C−N bond breaks and reforms repeatedly. The oxacarbenium ion intermediate has a finite lifetime in the active site before water attacks in the first irreversible step to complete the reaction. The lifetime of an oxacarbenium ion in solution is ~10^{-11} to 10^{-10} s.[13] There is no evidence for its lifetime in the MutY active site, but given the small barrier to nucleophilic attack[36] and the presence of both the leaving group adenine and the water nucleophile, it is likely to be fleeting. The dominant mechanism for acid-catalyzed dAMP hydrolysis was also $D_N*A_N^{\ddagger}$, and the quality of the match of calculated to experimental KIEs was similar.[13]

Individual KIEs. $1'$-^{14}C KIE. The experimental $1'$-^{14}C KIE, 1.009, reflects normal contributions from loss of the C1′−N9 bond and the reaction coordinate, offset by a large inverse contribution from the extensive π-bonding to O4′ and C2′. The inverse contribution is large enough that the calculated $1'$-^{14}C EIE for oxacarbenium ion formation was inverse. The reaction coordinate contribution in $8a^{\ddagger}/8b^{\ddagger}$ is relatively modest because of the weak C1′−O bond and low mass of the water nucleophile. This results in a smaller $1'$-^{14}C KIE than for a $D_N^{\ddagger}*A_N$ mechanism ($5^{\ddagger}$) or A_ND_N mechanism ($4^{\ddagger}$), where the stronger C1′−N9 (and C1′−O) bonds and the mass of the leaving group (and nucleophile) give larger reaction coordinate contributions and therefore larger calculated $1'$-^{14}C KIEs.

9-^{15}N KIE. The large 9-^{15}N KIE indicated complete C−N bond cleavage at the transition state. The calculated 9-^{15}N KIEs for the $D_N^{\ddagger}*A_N$ and A_ND_N mechanisms were too large, due to the contribution from the reaction coordinate motion. Thus, the 9-^{15}N KIE further supported a $D_N*A_N^{\ddagger}$ (or $D_N*?^{\ddagger}$) mechanism.

7-^{15}N KIE. The inverse 7-^{15}N KIE showed that N7 is protonated at the transition state. This is definitive evidence for general acid catalysis through N7, consistent with the fact that eMutY cannot hydrolyze 7-deaza-adenine substrates even though they are intrinsically more reactive than adenine.[37] Up to 7 kcal/mol of catalytic enhancement is possible from N7 protonation.[7,38] If MutY were to take full advantage of the catalytic effect of N7 protonation, that would account for more than half of its catalytic power. The calculated 7-^{15}N KIEs were all similar to each other, and thus did not distinguish between the alternative mechanisms.

(33) Guthrie, R. D.; Jencks, W. P. *Acc. Chem. Res.* **1989**, *22*, 343–349.
(34) Berti, P. J. *Methods Enzymol.* **1999**, *308*, 355–397.
(35) Scott, A. P.; Radom, L. *J. Phys. Chem.* **1996**, *100*, 16502–16513. Wong, M. W. *Chem. Phys. Lett.* **1996**, *256*, 391–399.

(36) Richard, J. P.; Williams, K. B.; Amyes, T. L. *J. Am. Chem. Soc.* **1999**, *121*, 8403–8404.
(37) Porello, S. L.; Williams, S. D.; Kuhn, H.; Michaels, M. L.; David, S. S. *J. Am. Chem. Soc.* **1996**, *118*, 10684–10692. Lu, A. L.; Tsai-Wu, J. J.; Cillo, J. *J. Biol. Chem.* **1995**, *270*, 23582–23588. (b) Francis, A. W.; Helquist, S. A.; Kool, E. T.; David, S. S. *J. Am. Chem. Soc.* **2003**, *125*, 16235–16242.
(38) Kampf, G.; Kapinos, L. E.; Griesser, R.; Lippert, B.; Sigel, H. *J. Chem. Soc., Perkin Trans. 2* **2002**, 1320–1327.
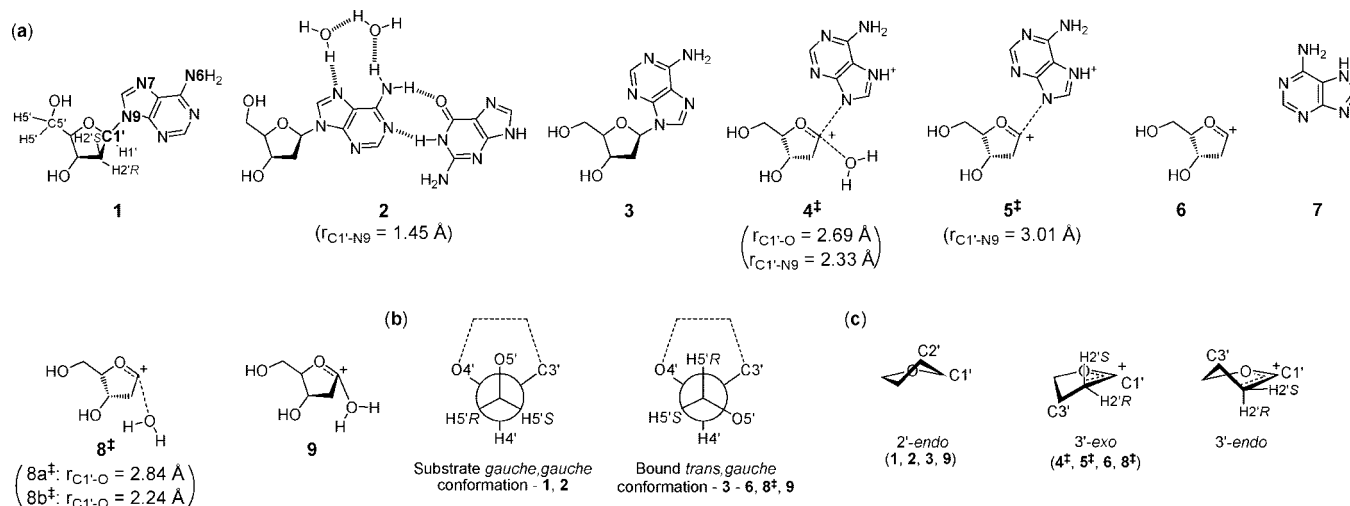
Figure 3. Structures for calculating KIEs. (a) Unpaired reactant dAdo (**1**), reactant dAdo in a G:A mismatch (**2**), enzyme bound reactant (**3**), transition states (**4‡**, **5‡**, **8‡**), intermediates (**6**, **7**), and the protonated product (**9**). Transition state and intermediate structures were developed from **3**. The effect on KIEs of neglecting the 5′-phosphate in calculations was negligible.[13] (b) Structures **1** and **2** were gauche,gauche conformers about the C4′-C5′ bond, while **3** - **9** were trans,gauche. (c) The 2′-endo or 3′-exo sugar ring conformations are shown, along with the hypothetical 3′-endo conformer.[43] (See Supporting Information for the Cartesian coordinates of **1** to **9** (Table S9), and a summary of the sugar ring geometries of **6**, **8a‡**, and **8b‡** (Table S7).)

Table 2. Comparison of Experimental and Calculated KIEs for Different Mechanisms of dAdo Hydrolysis[a]

	KIEs					
	$A_N D_N$	$D_N*?^{‡b}$	$D_N^{‡}*A_N$	$D_N*A_N^{‡}$		
isotopic label	**2 → 4‡**	**2 ⇌ 6 + 7**	**2 → 5‡**	**2 → 8a‡ + 7**	**2 → 8b‡ + 7**	experimental[c]
1′-^{14}C	1.037	0.997	1.018	1.012	1.008	1.009
9-^{15}N	1.029	1.024	1.031	1.024[d]	1.024[d]	1.025
7-^{15}N	0.996	0.991	0.993	0.991[d]	0.991[d]	0.992
6-^{15}N	1.014	1.008	1.016	1.008[d]	1.008[d]	1.011
1′-^{3}H	1.182	1.345	1.492	1.400	1.244	1.150
2′S-^{2}H	1.062	1.195	1.257	1.179	1.134	1.091
2′R-^{2}H	1.019	1.070	1.076	1.068	0.998	1.077
5′S,5′R-^{3}H	1.001	0.970	1.014	0.977	0.971	0.968

[a] See Supporting Information, Figure S1 for the kinetic mechanism of D_N*A_N mechanisms, and Tables S1 to S5 for reduced isotopic partition functions, Q and $Q^{‡}$, used to calculate IEs. [b] The observable KIEs for this mechanism are the same as the EIEs for formation of the oxacarbenium ion intermediate, **6**, and adenine, **7**. [c] From Table 1. [d] As the leaving group is not present in the A_N step, the KIE equals the EIE for adenine formation.

6-^{15}N KIE. The 6-^{15}N KIE, 1.011, was larger than for acid-catalyzed dAMP hydrolysis, 0.997.[13] This appears to be a consequence of the loss of hydrogen bonding to N6 at the transition state. Including guanine and solvating waters in **2**, the reactant model, gave a calculated 6-^{15}N KIE of 1.008, compared with 1.003 for **1**. In the bMutY_D144N:(OG:A) structure, there is a potential N6·water hydrogen bond, but no direct N6·protein contacts are evident. Thus, the experimental KIE reflects the loss of hydrogen bonding and/or solvation at N6 at the transition state. The lack of protein interactions is consistent with the modest 3-fold effect of removing N6 from the substrate.[39]

Solvent Deuterium KIE. The solvent deuterium KIE under single turnover conditions was 0.54 ± 0.18, similar to that for acid-catalyzed dAMP hydrolysis, 0.43.[40] The solvent deuterium KIE reflects the *rate-limiting* step because it was measured under noncompetitive conditions, that is, in either H_2O or D_2O.

Because single turnover conditions were used, that is, with [eMutY] > [GA25], the rate-limiting step was chemical catalysis rather than the overall rate-limiting step, namely, product release. Presumably the rate-limiting chemical step is C—N bond cleavage. Thus, the inverse KIE demonstrated that there is no proton transfer during C—N bond cleavage. We conclude that N7 is protonated in a pre-equilibrium step before C—N bond cleavage because (i) N7H-adenosine is stable enough in solution to be observed by NMR,[38] (ii) adenine anion is a poor leaving group, and (iii) N7 is protonated by the time of the A_N step.

^{2}H and ^{3}H KIEs. The best match of calculated to experimental ^{2}H and ^{3}H KIEs was with the $D_N*A_N^{‡}$ mechanism; however, as observed previously,[13] the agreement of calculated to experimental KIEs was not as close as for heavy atom KIEs. Nonetheless, the experimental KIEs agreed well with related N-glycoside reactions,[7,10,13,19,20,22,23] and can readily be interpreted empirically. The 1′-^{3}H KIE was large and normal, indicating high oxacarbenium ion character.[7] The 2′-^{2}H KIEs were large and normal, also demonstrating high oxacarbenium ion character. Large 2′-^{2}H KIEs arise from hyperconjugation,[41,42] that is, electron donation from the C2′-H2 σ-bonds into a C2′-C1′ π-bond, which weakens the σ-bonds. Hyperconjugation varies with the $\theta_{H2'}$ dihedral angle (∠p-orbital−C1′−C2′−H2′). It is maximal when $\theta_{H2'} = 0°$ or 180°, and zero at 90°. The experimental 2′S-^{2}H KIE, 1.091, was larger than the 2′R-^{2}H KIE, 1.077. Only a 3′-exo sugar ring conformation will give this pattern of KIEs.[43] In the computational model, **6**, $\theta_{H2'S} = 18°$, and $\theta_{H2'R} = 135°$. The 5′,5′-^{3}H$_2$ KIE was large and inverse, 0.968. The calculated EIE between structures **2** and **3** was 0.972, indicating that the dominant contributor to the experimental KIE
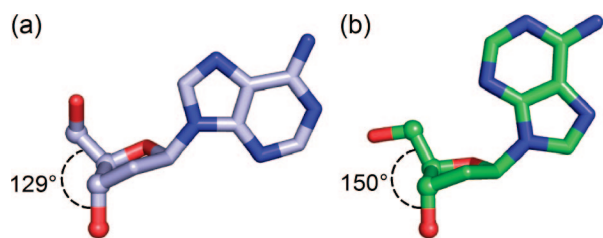
(39) Chmiel, N. H.; Golinelli, M. P.; Francis, A. W.; David, S. S. *Nucleic Acids Res.* **2001**, 29, 553–564.
(40) York, J. L. *J. Org. Chem.* **1981**, 46, 2171–2173.
(41) Matsson, O.; Westaway, K. C. *Adv. Phys. Org. Chem.* **1998**, 31, 143–248.
(42) Sunko, D. E.; Szele, I.; Hehre, W. J. *J. Am. Chem. Soc.* **1977**, 99, 5000–5004.
(43) Ring puckers are indicated by n-endo and n-exo designations, where all ring atoms except n are in the same plane. Atom n is displaced toward the 5′-substituent in n-endo conformers, and away in n-exo. IUPAC-IUB Joint Commission on Biochemical Nomenclature. Abbreviations and symbols for the description of conformations of polynucleotide chains. *Pure Appl. Chem.* **1983**, 55, 1273–1280.

Figure 4. (a) Typical dAdo residue in B-DNA (PDB: 1FQ2); (b) target dAdo residue in bMutY_D144N·(OG:A) (PDB: 1RRQ).[9] The atoms defining δ ($\angle C5'-C4'-C3'-O3'$) are shown as small spheres. (See Supporting Information for all backbone δ angles surveyed (Table S8).)

was the conformational change when eMutY flips dAdo out of the DNA base stack and into its active site.

Comparison with Acid-Catalyzed dAMP Hydrolysis. The nonenzymatic analogue of the MutY reaction is acid-catalyzed dAMP hydrolysis. Our recent TS analysis demonstrated that the acid-catalyzed reaction proceeded through the same stepwise $D_N*A_N^\ddagger$ mechanism, with reversible C−N bond cleavage followed by irreversible water attack on the oxacarbenium ion.[13] The lifetime of the oxacarbenium ion intermediate was on the same order as diffusional separation of the ion pair complex, 10^{-11} to 10^{-10} s. The structures $8a^\ddagger$ and $8b^\ddagger$ were effectively the same as the corresponding models of dAMP hydrolysis (also numbered $8a^\ddagger$ and $8b^\ddagger$ in reference 13). The main difference was in the γ-dihedral angle ($\angle O5'-C5'-C4'-C3'$), which, in the present study, reflected the conformation of dAdo flipped out of the DNA base stack by MutY. Despite the very similar structures, the experimental KIEs were quite distinct (Table 1). The difference in heavy atom KIEs arose primarily from the difference in protonation states. In acid-catalyzed hydrolysis, dAMP was protonated at N1 ($pK_a \approx 3.7$) in the reactant state, and the transition state was diprotonated, at N1 and N7. Thus, the C−N bond was weaker in the reactant, which was reflected in the smaller $1'-^{14}C$. These differences were also reflected in the calculated KIEs for acid-catalysis, which were also distinct from the eMutY KIEs, and matched the experimental KIEs for the acid-catalyzed reaction very well.

The $1'-^3H$ KIE was larger in the acid-catalyzed reaction.[13] This could reflect greater steric constraint in the enzyme active site, though the general difficulty in interpreting α-secondary KIEs argues against more a detailed interpretation.[41] The stereospecific $2'-^2H$ KIEs were similar in size to the eMutY-catalyzed reaction, and also indicated a 3'-*exo* conformation at the transition state. The $5',5'-^3H_2$ KIE was small and normal, as would be expected in the absence of a conformational change enforced by the enzyme.

Nucleotide Backbone Distortion. MutY appears to cause two types of DNA distortion. It flips dAdo out of the base stack into an extrahelical conformation, as seen in the crystal structure and in the $5',5'-^3H_2$ KIE. Comparing the bMutY-bound target dAdo residue with 54 other high resolution crystal structures also revealed that it distorts the sugar ring to stabilize the oxacarbenium ion. This is apparent in the δ dihedral angle ($\angle C5'-C4'-C3'-O3'$), which is intimately linked to the DNA backbone conformation (Figure 4). In undistorted dAdo residues, $\delta = 130° \pm 18°$. Members of the HhH superfamily of DNA glycosylases had $\delta = 152° \pm 6°$ in the target residue in substrates,[44,45] and intermediate and product analogues.[44,46] In

bMutY, $\delta = 150°$. The computational models **6**, $8a^\ddagger$, and $8b^\ddagger$ had $\delta = 149° \pm 1°$, compared with $142° \pm 1°$ in **2** and **1**. Thus, although possibly a modest effect, HhH enzymes bind substrates in a conformation that favors oxacarbenium ions, or oxacarbenium ion-like transition states. This is an example of ground-state destabilization.

Discussion

TS analysis provides a number of insights into the eMutY mechanism. The inverse $7-^{15}N$ KIE demonstrates that the reaction is general acid-catalyzed at N7. Adenine departure in the anion form ($pK_a = 9.7$)[47] is difficult but not impossible, as illustrated by 5'-methylthioadenosine phosphorylase.[10] Also, UDG catalyzes uracil departure in the anion form.[21] However, nonenzymatic purine hydrolysis is acid-catalyzed because protonated bases are much better leaving groups, and eMutY clearly takes advantage of this by protonating N7, which has a microscopic $pK_a \approx 2.4$,[7] to promote leaving group departure.

The reaction proceeds through a $D_N*A_N^\ddagger$ mechanism. This does not merely imply that the C−N bond breaks and reforms repeatedly. The fact that commitment to catalysis is negligible means that when the highly reactive oxacarbenium ion intermediate is formed, the most probable outcome is that the C−N bond will reform, N7 will be deprotonated, and the eMutY•GA25 complex will dissociate to the free molecules in solution.

TS analysis demonstrated that the oxacarbenium ion intermediate exists in the 3'-*exo* conformation, in contrast to DNA's usual 2'-*endo* conformation (Figure 3c). Nonenzymatic and most enzymatic reactions proceed through transition states or oxacarbenium ions in the 3'-*exo* conformation, and only the 3'-*exo* conformer is stable computationally.[7] Thus, eMutY places the oxacarbenium ion in its most favored conformation, and there is some evidence that it distorts the target dAdo residue to achieve this, as reflected in the dihedral angle δ. In contrast, ricin-catalyzed DNA hydrolysis had a larger $2'R-^2H$ KIE than $2'S-^2H$ KIE, indicating that it proceeded through a 3'-*endo* ring conformation.[23] This was a consequence of the substrate's backbone conformation, with the target A residue being part of the GAGA loop in a stem-loop substrate. KIE and structural studies indicated that UDG enforces a flattened 3'-*exo* geometry in the oxacarbenium ion intermediate.[21]

Individual Steps of Catalysis. While TS analysis on its own provides a detailed view of catalysis, combining it with the bMutY_D144N·(OG:A) crystal structure creates a step-by-step picture of the catalytic cycle. These structures represent the starting and ending points of the chemical steps of catalysis. The crystal structure is an abortive Michaelis complex after OG:A has been recognized, the DNA backbone distorted, and dAdo flipped into the active site. The D144N mutation prevents catalysis but did not meaningfully alter the active site structure, as shown by the fact that the Asn144 side chain superimposed on wild-type Asp144. The experimental TS structure is the last step of catalysis, that is, water attack on the oxacarbenium ion intermediate. These structures are reference points; combining them makes it possible to present a step-by-step catalytic sequence (Figure 5, and Movie S1).

(44) Norman, D. P.; Chung, S. J.; Verdine, G. L. *Biochemistry* **2003**, *42*, 1564–1572.
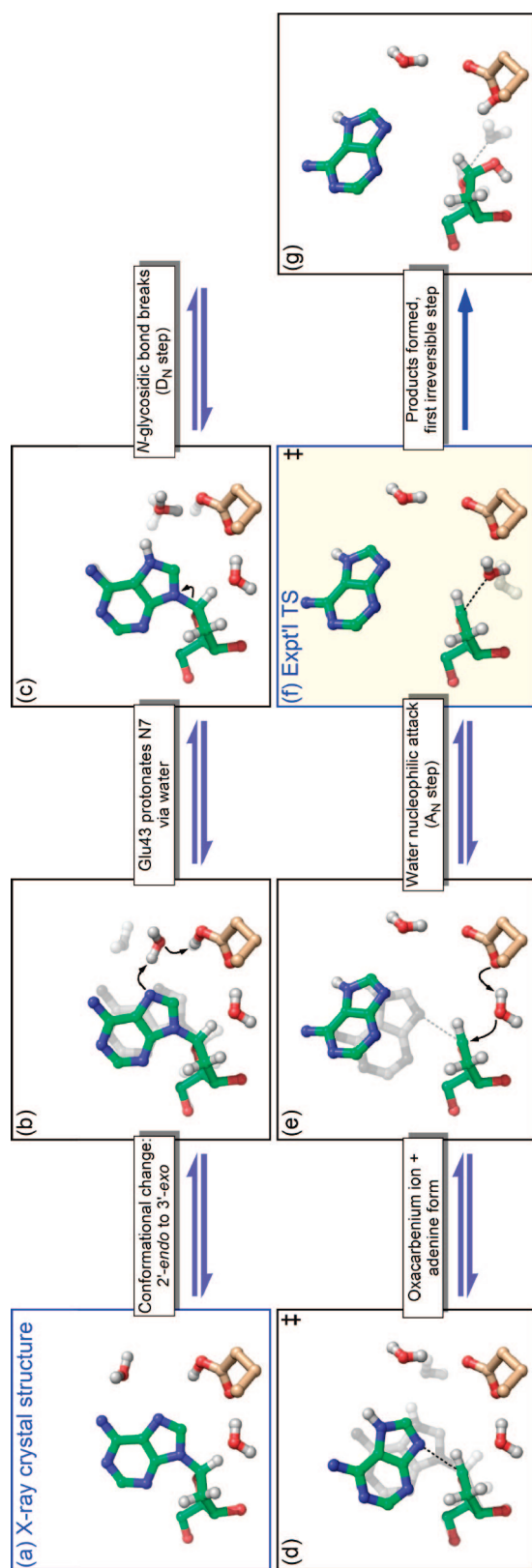
(45) Bruner, S. D.; Norman, D. P.; Verdine, G. L. *Nature* **2000**, *403*, 859–866.

(46) Hollis, T.; Ichikawa, Y.; Ellenberger, T. *EMBO J.* **2000**, *19*, 758–766. Norman, D. P. G.; Bruner, S. D.; Verdine, G. L. *J. Am. Chem. Soc.* **2001**, *123*, 359–360.

(47) Martin, R. B. *Acc. Chem. Res.* **1985**, *18*, 32–38.

Figure 5. Proposed catalytic mechanism for MutY. An animation of the catalytic mechanism is included as a movie. The crystal structure (**a**) and the experimental TS structure (**f**) are the reference points for the proposed mechanism. In each panel, the previous structure is shown in light grey. Every step before **f** is reversible. (**a**) dAdo, Glu43, Wat17 (proton relay), and Wat10 (nucleophile) from the bMutY_D144N•(OG:A) crystal structure.[9] (**b**) dAdo in the 3′-exo conformation and Wat17 positioned to transfer a proton from Glu43 to N7. (**c**) N7H-dAdo after protonation. (**d**) Computational transition state, **5**‡, for C−N bond cleavage, the D$_N$ step. (**e**) Oxacarbenium ion + adenine intermediate, structures **6** + **7**. (**f**) Experimental TS structure, water attack on the oxacarbenium ion intermediate, structures **8a**‡ + **7**. The timing of general base catalysis relative to nucleophilic attack is not known. (**g**) AP-DNA product. Relevant structures from Figure 3 were used where possible, otherwise the dAdo residue was optimized at the same level of theory, B3PW91/6−31+G**.[13] In panels **b** and **c**, dAdo was constrained to be the 3′-exo conformer. The protons on Wat10, Wat17 and Glu43 were optimized at the semiempirical, AM1, level. The heavy atoms of Glu43, plus dAdo O5′, C5′, C4′, C3′ and O3′ were fixed as in the crystal structure. A movie showing the catalytic sequence for MutY is available.

Conformational Change/Water Movement. The target dAdo had a 2'-*endo*[43] sugar ring pucker in the crystal structure, typical of DNA. The transition state was a 3'-*exo* conformer, which is rare in DNA but the most common oxacarbenium ion conformer. There is no experimental evidence for when this conformational change occurs; however, proposing it as the first step solves a problem with general acid catalysis. E37/43 was proposed to be the general acid catalyst that protonates N7,[8,9] but it was too far from N7 in the crystal structure to protonate it directly (Figure 5, panel a). Two crystallographic waters were proposed as potential proton relays, but Wat17 was 4.2 Å from Glu43 and Wat60 was not coplanar with the adenine ring. Changing the dAdo conformation from 2'-*endo* to 3'-*exo* moves the adenine ring away from Glu43, creating enough space between N7 and Glu43 Oϵ for a water molecule to move and hydrogen bond to both then relay a proton from Glu43 to N7 (Wat17 is shown, but either is possible). Given the numerous phosphate backbone contacts, the conformational change would more likely cause the adenine ring to move rather than the DNA backbone. The conformational change would be energetically facile; C1' simply moves upward and N7 moves away from E37/43 by 0.6 Å (panel a → b).

N7 Protonation. The 7-^{15}N KIE demonstrates that N7 is protonated, and the solvent deuterium KIE indicates that this occurs before C−N bond cleavage. The repositioned water is proposed to relay a proton from E37/43 to N7 (panel b → c).

C−N Bond Cleavage. After N7 protonation the C−N bond breaks, passing through the D_N step transition state (panel d) to form the oxacarbenium ion + adenine intermediate (panel e). TS structure **5**‡ is shown; however, KIEs in a D_N*A_N‡ mechanism contain no experimental information on the D_N step. Once the C−N bond is broken, the location of adenine in the active site is unknown, but because C−N cleavage is reversible, it must be available to reform the C−N bond until after the transition state for water addition. If it were not available, C−N cleavage would be irreversible and the KIEs would reflect a different mechanism.

C−O Bond Formation. C−O bond formation in the A_N step (panel f) is the first irreversible step. Forming the C1'-O bond (panel g) completes the chemical steps of the reaction. The water nucleophile of **8a**‡ (panel f) almost superimposed on Wat10 in bMutY_D144N·(OG:A) (panel e), the proposed nucleophile. Wat10 was located 2.2 Å from E37/43 Oϵ, the proposed general base.[9] Similar crystallographic waters occur in the other MutY structures.[8,48]

Although E37/43 has been proposed to be a base catalyst, one could argue, given the exceedingly small barrier to nucleophilic attack on oxacarbenium ions[36] and the acidity of the protonated product, **9**, that it may not be necessary. However, the fact that most or all *O*- and *N*-glycosylases appear to possess a general base catalytic residue positioned to deprotonate the water nucleophile, suggests that base catalysis is important.[7] The timing of general base catalysis is not known, whether it occurs before, during, or after nucleophilic attack by water.

Postchemistry Steps. Adenine dissociation from eMutY·adenine·AP-DNA is relatively fast, >5 min^{-1}.[49] AP-DNA product dissociation is by far the rate-limiting step for eMutY, at 0.005 min^{-1} for (OG:AP)-DNA, and 0.03 min^{-1} for (G:AP)-DNA.[25,49] There is evidence that dissociation can be accelerated by AP endonuclease, the next enzyme in the base excision repair pathway.[50]

Transition States of Related Reactions. The experimental KIEs for hydrolysis of uracil from DNA by UDG[21] and adenine from DNA by ricin (the normal substrate is RNA)[23] also indicated stepwise mechanisms. The original reports could not distinguish which was the first irreversible step. We argued recently, based on expanded computational models, that the 1'-^{14}C KIEs indicate D_N‡*A_N mechanisms for both reactions, where C−N bond cleavage is the first irreversible step.[13] That is, an oxacarbenium ion intermediate is formed, as with eMutY, but the C−N bond does not reform. The reason for this difference is not known. Ricin-catalyzed adenine hydrolysis from RNA was also stepwise, but in this case the first irreversible step was an unknown isotopically insensitive step after intermediate formation.[22] This unknown step could be, for example, a protein conformational change, or water diffusion into position to attack the intermediate.

TS analyses of small molecule *N*-glycosylase reactions most commonly indicate highly dissociative A_ND_N (S_N2) transition states with oxacarbenium ion-*like* transition states, but no discrete intermediate species.[7] Recently, a small number of stepwise mechanisms have been observed.[10,19,20] The fact that the nucleic acid *N*-glycosylases studied to date, namely UDG,[21] ricin,[22,23] and MutY, all proceed through stepwise mechanisms is not surprising, given the fact that the corresponding acid-catalyzed reaction, dAMP hydrolysis, also proceeds through a stepwise D_N*A_N‡ mechanism.[13] MutY stabilizes the same transition state as the acid-catalyzed reaction; however, there is no reason *a priori* to expect this to be the case. Many enzymes stabilize different transition states than the corresponding nonenzymatic reactions. Various *O*-glycosidases, for example, would hydrolyze the same *O*-glycoside substrate by direct nucleophilic displacement (the inverting glycosidases), through a covalent acyl-enzyme intermediate (the retaining glycosidases),[51] or by transient oxidization of a hydroxyl group to a ketone two positions away from the scissile bond.[52]

In *N*-glycoside chemistry, TS analyses of malarial, bovine, and human purine nucleoside phosphorylases indicated subtly, but measurably, different transition states despite very similar catalytic sites.[19,53] These differences were corroborated by differences in K_d's of inhibitors that mimic different transition state structures.[17,54] Thymidine phosphorylase stabilizes a remarkable, almost synchronous A_ND_N transition state with essentially no oxacarbenium ion character, a radical departure from the nonenzymatic reaction.[24] We still cannot predict which transition state a particular enzyme will stabilize, but as in the

(48) Manuel, R. C.; Hitomi, K.; Arvai, A. S.; House, P. G.; Kurtz, A. J.; Dodson, M. L.; McCullough, A. K.; Tainer, J. A.; Lloyd, R. S. *J. Biol. Chem.* **2004**, *279*, 46930–46939.

(49) McCann, J. A. B.; Berti, P. J. *J. Biol. Chem.* **2003**, *278*, 29587–29592.

(50) Pope, M. A.; Porello, S. L.; David, S. S. *J. Biol. Chem.* **2002**, *277*, 22605–22615.

(51) Zechel, D. L.; Withers, S. G. *Acc. Chem. Res.* **2000**, *33*, 11–18. Davies, G.; Sinnott, M. L.; Withers, S. G. In *Comprehensive Biological Cataysis*; Sinnott, M., Ed.; Academic Press: London, 1997; p 120−209.

(52) Yip, V. L. Y.; Varrot, A.; Davies, G. J.; Rajan, S. S.; Yang, X.; Thompson, J.; Anderson, W. F.; Withers, S. G. *J. Am. Chem. Soc.* **2004**, *126*, 8354.

(53) Schramm, V. L. *J. Biol. Chem.* **2007**, *282*, 28297–28300.

(54) Lewandowicz, A.; Shi, W. X.; Evans, G. B.; Tyler, P. C.; Furneaux, R. H.; Basso, L. A.; Santos, D. S.; Almo, S. C.; Schramm, V. L. *Biochemistry* **2003**, *42*, 6057–6066. Evans, G. B.; Furneaux, R. H.; Lewandowicz, A.; Schramm, V. L.; Tyler, P. C. *J. Med. Chem.* **2003**, *46*, 5271–5276.

case of MutY, determining TS structures opens the door to highly detailed mechanistic analyses.

Conclusions

TS analysis demonstrated that eMutY catalyzes adenine hydrolysis through a stepwise $D_N^*A_N^\ddagger$ (S_N1) mechanism. It catalyzes reversible oxacarbenium ion formation, followed by irreversible water attack to complete the chemical steps of the reaction. It appears that substrate binding is accompanied by ground-state destabilization through sugar ring distortion to stabilize an oxacarbenium ion intermediate over the reactant, as evident in the dihedral angle δ. A further conformational change from the 2′-*endo* to 3′-*exo* conformer allows water to bridge between N7 and E37/43, the general acid catalyst. N7 is protonated, followed by C−N bond cleavage to form an oxacarbenium ion intermediate. The water nucleophile then attacks the oxacarbenium ion and is deprotonated, completing catalysis.

Supporting Information Available: Description of C_f measurement; details of GA25 synthesis and purification; chromatogram from KIE measurement; complete tables for IEs calculations; influence of hydration and hydrogen bonding on IEs; summary of sugar ring geometries; backbone δ angles surveyed; Cartesian coordinates of optimized structures. This material is available free of charge via the Internet at http://pubs.acs.org.

JA711363S